

LETTER TO THE EDITOR

Detection of chloronium and measurement of the $^{35}\text{Cl}/^{37}\text{Cl}$ isotopic ratio at $z = 0.89$ toward PKS 1830–211

S. Muller¹, J. H. Black¹, M. Guélin^{2,3}, C. Henkel^{4,5}, F. Combes⁶, M. Gérin³, S. Aalto¹, A. Beelen⁷, J. Darling⁸, C. Horellou¹, S. Martín², K. M. Menten⁴, Dinh-V-Trung⁹, and M. A. Zwaan¹⁰

¹ Department of Earth and Space Sciences, Chalmers University of Technology, Onsala Space Observatory, 43992 Onsala, Sweden
e-mail: mullers@chalmers.se

² Institut de Radioastronomie Millimétrique, 300 rue de la piscine, 38406 St-Martin d'Hères, France

³ LRA/LERMA, CNRS UMR 8112, Observatoire de Paris & École Normale Supérieure, 75231 Paris, France

⁴ Max-Planck-Institut für Radioastronomie, Auf dem Hügel 69, 53121 Bonn, Germany

⁵ Astron. Dept., King Abdulaziz University, PO Box 80203, 21589 Jeddah, Saudi Arabia

⁶ Observatoire de Paris, LERMA, CNRS, 61 Av. de l'Observatoire, 75014 Paris, France

⁷ Institut d'Astrophysique Spatiale, Bât. 121, Université Paris-Sud, 91405 Orsay Cedex, France

⁸ Center for Astrophysics and Space Astronomy, Department of Astrophysical and Planetary Sciences, University of Colorado, 389 UCB, Boulder, CO 80309-0389, USA

⁹ Institute of Physics, Vietnam Academy of Science and Technology, 10 DaoTan, ThuLe, BaDinh, Hanoi, Vietnam

¹⁰ European Southern Observatory, Karl-Schwarzschild-Str. 2, 85748 Garching b. München, Germany

Received 4 April 2014 / Accepted 28 April 2014

ABSTRACT

We report the first extragalactic detection of chloronium (H_2Cl^+) in the $z = 0.89$ absorber in front of the lensed blazar PKS 1830–211. The ion is detected through its $1_{11}-0_{00}$ line along two independent lines of sight toward the North-East and South-West images of the blazar. The relative abundance of H_2Cl^+ is significantly higher (by a factor ~ 7) in the NE line of sight, which has a lower H_2/H fraction, indicating that H_2Cl^+ preferably traces the diffuse gas component. From the ratio of the $\text{H}_2^{35}\text{Cl}^+$ and $\text{H}_2^{37}\text{Cl}^+$ absorptions toward the SW image, we measure a $^{35}\text{Cl}/^{37}\text{Cl}$ isotopic ratio of $3.1^{+0.3}_{-0.2}$ at $z = 0.89$, similar to that observed in the Galaxy and the solar system.

Key words. quasars: absorption lines – galaxies: ISM – galaxies: abundances – ISM: molecules – radio lines: galaxies – quasars: individual: PKS 1830-211

1. Introduction

A plethora of new interstellar molecules, notably simple hydrides, has been discovered as a result of the recent opening of the submillimeter window, from space with the *Herschel* Space Observatory, or from the ground, for example with the Atacama Pathfinder EXperiment (APEX) and Caltech Submillimeter Observatory (CSO) telescopes. Hydrides (that is, molecular species composed of a single heavy element with one or more hydrogen atoms) are formed by the first chemical reactions in the atomic gas component, and are therefore at the basis of interstellar chemistry. They are powerful probes of the interstellar environment and offer a variety of astrophysical diagnostics (e.g., Qin et al. 2010; Gerin et al. 2010; Godard et al. 2012; Flagey et al. 2013; Schilke et al. 2014).

One such hydride is chloronium, H_2Cl^+ , which was first detected by Lis et al. (2010) in foreground absorption toward the sources NGC 6334I and Sgr B2(S) with the Herschel Space Observatory. Neufeld et al. (2012) extended observations of H_2Cl^+ to six Galactic sources, four in absorption and two in emission (toward OMC 1: Orion Bar and Orion South). These constitute the only observations of chloronium in the literature to date. The other chlorine-bearing molecules detected in the interstellar medium are hydrogen chloride, HCl (Blake et al. 1985) and the chloroniumyl ion, HCl^+ (de Luca et al. 2012), while

metal halides such as NaCl, AlCl, and KCl were detected in the circumstellar envelope IRC+10216 (Cernicharo & Guélin 1987) and in the atmosphere of Io (Lellouch et al. 2003; Moullet et al. 2010, 2013).

Here, we report the first extragalactic detection of chloronium, in the $z = 0.89$ absorber toward the $z = 2.5$ blazar PKS 1830–211, and a measurement of the $^{35}\text{Cl}/^{37}\text{Cl}$ isotopic ratio at a look-back time of more than half the present age of the Universe.

2. Data

The $1_{11}-0_{00}$ line of the para spin-species of both the $\text{H}_2^{35}\text{Cl}^+$ and $\text{H}_2^{37}\text{Cl}^+$ isotopologues, with rest frequencies of ~ 485.4 GHz and ~ 484.2 GHz, respectively, was detected in absorption at $z_{\text{abs}} = 0.89$ (i.e., redshifted to ~ 257 GHz) toward the blazar PKS 1830–211 with the Atacama Large Millimeter/submillimeter Array (ALMA). The observations and details of the data reduction are described by Muller et al. (2014, hereafter Paper I). We used ALMA Band 6 data from four observing runs performed between April and June 2012. The total resulting on-source integration time was approximately 30 min. The two lensed images of the background blazar, separated by $1''$, were resolved by the ALMA array, but each remained a point-like source. One absorption spectrum was extracted toward

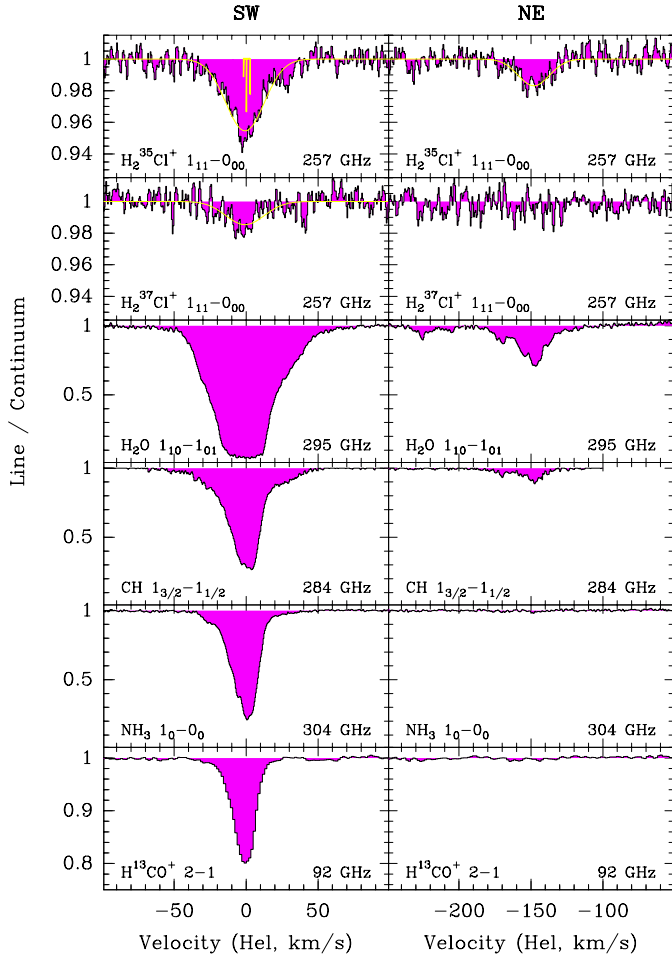


Fig. 1. Spectra of the $\text{H}_2^{35}\text{Cl}^+$ and $\text{H}_2^{37}\text{Cl}^+$ $1_{11}-0_{00}$ (para) line and other species, all observed by ALMA between April and June 2012, toward the PKS 1830–211 SW image (*left*) and the NE image (*right*). The hyperfine structure for the $\text{H}_2^{35}\text{Cl}^+$ para-line is shown (*top-left*). That for $\text{H}_2^{37}\text{Cl}^+$ is similar. The Gaussian fits are overlaid in light yellow. The redshifted line frequency is given in the *bottom-right* corner of each box. A detailed presentation of the ALMA data is given by Muller et al. (2014).

each image with the task UVMULTIFIT (Martí-Vidal et al. 2014), by modelling the visibilities with two point-like sources where the relative positions were fixed and the flux densities left as free parameters. The two chloronium isotopologues were observed simultaneously in the same spectral window, 1.875 GHz wide and with a spectral channel spacing of 0.488 MHz. The resulting velocity resolution of the chloronium spectra is 1.2 km s^{-1} after Hanning smoothing.

The chloronium frequencies and relative intensities of the hyperfine components are taken from the work by Araki et al. (2001). The dipole moment, $\mu = 1.89 \text{ D}$, is from an ab initio calculation by Müller (2008). All velocities are referred to redshift $z = 0.88582$ in the heliocentric frame.

The absorption of $\text{H}_2^{35}\text{Cl}^+$ is detected toward both images of the blazar while that of $\text{H}_2^{37}\text{Cl}^+$ is detected only toward the SW image (see Fig. 1). The lines are shallow and optically thin toward both images, absorbing only a few percent of the continuum background. Because the width of the absorption profile is larger than the splitting of the hyperfine structure (over $\sim 4.5 \text{ km s}^{-1}$, as shown in Fig. 1), we did not deconvolve the spectra.

3. Discussion

3.1. Column densities and abundances

Chloronium is a widespread species in the Galactic diffuse medium (Neufeld et al. 2012), and it is not surprising to detect it in the SW absorption toward PKS 1830–211. Indeed, the SW line of sight is particularly rich in molecules, with more than 40 species detected to date (Muller et al. 2011 and Paper I). What is surprising at first glance, however, is to detect chloronium absorption toward the NE image, with a SW/NE absorption depth ratio of only 3–4, while all other molecular species observed so far have a much deeper absorption toward the SW image, with SW/NE abundance ratios of a few tens (e.g., Muller et al. 2011). This is well illustrated in Fig. 1 by the comparison of the chloronium absorption toward both images with the absorption from species such as H_2O , CH , NH_3 , and H^{13}CO^+ . All spectra were observed by ALMA between April and June 2012 and are not affected by time variations (see Muller & Guélin 2008 and the discussion in Paper I). Note that the H_2O absorption is heavily saturated toward the SW image. Only the H I line (e.g., Koopmans & de Bruyn 2005) shows an absorption deeper (by a factor ~ 2) toward the NE image than toward the SW image.

The line profile of the $\text{H}_2^{35}\text{Cl}^+$ absorption toward the SW image is wider ($FWHM = 32 \pm 1 \text{ km s}^{-1}$) than that of the optically thin H^{13}CO^+ 2–1 line ($FWHM = 17.1 \pm 0.3 \text{ km s}^{-1}$). In particular, the $\text{H}_2^{35}\text{Cl}^+$ absorption shows an additional weak feature at a velocity of $\sim 30 \text{ km s}^{-1}$, where the H_2O and CH profiles have a prominent line wing, which most likely represents a diffuse gas component (see the discussion in Paper I).

We estimate an integrated opacity of $\sim 1.5 \text{ km s}^{-1}$ along the SW line of sight for the $\text{H}_2^{35}\text{Cl}^+$ -para line. Assuming a rotation temperature locked to the temperature of the cosmic microwave background, $T_{\text{CMB}} = 5.14 \text{ K}$ at $z = 0.89$ (see Muller et al. 2013), a source-covering factor f_c of unity, and an ortho/para ratio of 3 (Gerin et al. 2013), we derive a column density of $\sim 1.4 \times 10^{13} \text{ cm}^{-2}$. In fact, the covering factor of the SW image is not unity, but $\sim 95\%$, as shown by the saturation level of the 557 GHz water line (see Paper I). However, this does not introduce a noticeable difference in the apparent opacity of H_2Cl^+ since the line is optically thin and $f_c \sim 1$. With the same assumptions along the NE line of sight, we estimate an integrated opacity of $\sim 0.4 \text{ km s}^{-1}$, corresponding to a $\text{H}_2^{35}\text{Cl}^+$ column density of $4 \times 10^{12} \text{ cm}^{-2}$. With total H_2 column densities of 2×10^{22} and $1 \times 10^{21} \text{ cm}^{-2}$ along the SW and NE lines of sight, respectively (Muller et al. 2011 and Paper I), we finally derive fractional abundances of $[\text{H}_2^{35}\text{Cl}^+]/[\text{H}_2] \sim 6 \times 10^{-10}$ (SW) and $\sim 4 \times 10^{-9}$ (NE), that is, a H_2Cl^+ abundance relative to $\text{H}_2 \sim 7$ higher along the NE line of sight. Note that the covering factor is not well known toward the NE image, but the ALMA data suggest $0.3 < f_c < 1.0$. Assuming $f_c < 1$ would increase the true opacity, column density, and relative abundance of H_2Cl^+ , and give an even higher relative abundance ratio than for the SW line of sight.

The chemistry of interstellar chlorine is thought to be simple and well understood (see Neufeld & Wolfire 2009); but the observed abundances of the ions HCl^+ and H_2Cl^+ in the Galactic interstellar medium are rather higher than predicted in current models (Neufeld et al. 2012). In diffuse clouds, the chemistry starts from ionized chlorine (the first ionization potential of chlorine, 12.97 eV, is slightly lower than that of hydrogen), forming HCl^+ by reaction with H_2 . A further reaction of HCl^+ with H_2 leads to H_2Cl^+ . The molecule can in turn react with free electrons (dissociative recombination) to form HCl or Cl . In dense

Table 1. Astronomical measurements of the ³⁵Cl/³⁷Cl ratio.

Source	³⁵ Cl/ ³⁷ Cl	Species	Ref.
Solar system	3.13	Cl	1
IRC+10216	2.3 ± 0.5	NaCl, AlCl	2
Ori A	~4–6	HCl	3
IRC+10216	3.1 ± 0.6	NaCl, KCl, AlCl	4
IRC+10216	2.30 ± 0.24	NaCl, AlCl	5
W3 A [†]	2.1 ± 0.5	HCl	6
NGC 6334I, Sgr B2(S) [†]	~2.7–3.3	H ₂ Cl ⁺ and HCl	7
10 Galactic sources	~1–5 [‡]	HCl	8
W31 C, Sgr A [†]	~2–4	H ₂ Cl ⁺	9
W31 C [†]	2.1 ± 1.5	HCl ⁺	10
W31 C [†]	~2.9	HCl	11
CRL 2136	2.3 ± 0.4 [°]	HCl	12
PKS 1830–211(SW) [†]	3.1 ^{+0.3} _{-0.2}	H ₂ Cl ⁺	13
PKS 1830–211(NE) [†]	>1.9 [*]	H ₂ Cl ⁺	13

Notes. (†) The line was detected in absorption against the background source. (‡) Possible confusion between absorption and emission features. (°) A CH feature might partially blend with the H³⁷Cl signal, possibly affecting the derived value of the ratio. (*) At 99.7% confidence level.

References. (1) Lodders (2003); (2) Cernicharo & Guélin (1987); (3) Salez et al. (1996); (4) Cernicharo et al. (2000); (5) Kahane et al. (2000); (6) Cernicharo et al. (2010); (7) Lis et al. (2010); (8) Peng et al. (2010); (9) Neufeld et al. (2012); (10) de Luca et al. (2012); (11) Monje et al. (2013); (12) Goto et al. (2013); (13) this work.

clouds, the chemistry is driven by cosmic-ray ionization and not by UV-photoionization, and neutral chlorine can react with the H₃⁺ ion to form HCl⁺, which again can react with H₂ to produce H₂Cl⁺. The chemical rates and balance of the above reactions are not precisely known, but the relative abundance of H₂Cl⁺ clearly depends on the ionization level of chlorine, that is, on the UV irradiation field and atomic hydrogen density (Neufeld & Wolfire 2009).

The significantly higher relative abundance of H₂Cl⁺ in the NE line of sight, where the absorbing gas has a lower molecular fraction (H₂/H) than in the SW, confirms that the chloronium abundance is enhanced in the diffuse, more atomic, interstellar component (Neufeld et al. 2012).

3.2. ³⁵Cl/³⁷Cl isotopic ratio at $z = 0.89$

The clear detection of both H₂³⁵Cl⁺ and H₂³⁷Cl⁺ isotopologues toward the SW image allows us to measure their abundance ratio. The simple, well-known chlorine chemistry and the most likely weak fractionation between both isotopologues ensure that this ratio reflects the ³⁵Cl/³⁷Cl isotopic ratio. Note that both isotopologues were observed simultaneously and within the same 1.875 GHz-wide spectral window, which minimizes instrumental uncertainties. From a simultaneous fit of the SW spectrum with a single Gaussian component (centroid and width constrained to the same values for both isotopologues), we derive an isotopic ratio ³⁵Cl/³⁷Cl of 3.1^{+0.3}_{-0.2}, where uncertainties correspond to a 68% confidence level from a Monte Carlo analysis. If the ratio is the same toward the NE image, H₂³⁷Cl⁺ should be just at the limit of detection. We estimate a lower limit of ³⁵Cl/³⁷Cl > 1.9 at a 99.7% confidence level. Slightly deeper observations should thus allow us to measure the ³⁵Cl/³⁷Cl ratio toward this component, which intercepts the absorber at a larger galactocentric radius (~4 kpc vs. ~2 kpc for the SW image).

The measurement of ³⁵Cl/³⁷Cl at $z = 0.89$ (SW) is within the range of values found in Galactic sources (see Table 1), and is, in particular, identical to the terrestrial ratio within the uncertainty. In contrast to ³⁵Cl/³⁷Cl, the isotopic ratios of ¹⁸O/¹⁷O, ²⁸Si/²⁹Si, and ³²S/³⁴S in the same $z = 0.89$ absorber (SW line of sight) were found to deviate significantly by factors of 2–3 from their local Galactic values (see Muller et al. 2006, 2011, 2013). While little is known about the conditions of the $z = 0.89$ absorber (metallicity, elemental abundances, star formation activity), its look-back time is more than half the present age of the Universe. Consequently, we expect that the interstellar enrichment is more dominated by nucleosynthetic products from massive stars, especially concerning heavy elements such as silicon, sulfur, and chlorine, than a region with a similar galactocentric radius in the Milky Way.

The two stable isotopes of chlorine can be produced during hydrostatic oxygen burning from the α -elements ³²S and ³⁶Ar via ³²S(α, p)³⁵Cl and ³⁶Ar(n, γ)³⁷Ar(β^+)³⁷Cl, respectively (e.g., Thielemann & Arnett 1985). ³⁷Cl can also be produced from ³⁵Cl by s -process. ³⁶Cl is unstable, but its half-lifetime is of about 3×10^5 yr, long enough to catch a second neutron to reach ³⁷Cl before decay. In the interstellar gas, spallation reactions from cosmic rays on argon can also lead to chlorine isotopes.

In Fig. 2, we compare the isotopic ratios measured at $z = 0.89$ toward PKS 1830–211(SW) with theoretical predictions of time/metallicity evolution models by Kobayashi et al. (2011) in the Milky Way. For the solar neighbourhood, three epochs/metallicities are considered by Kobayashi et al. (2011): at [Fe/H] = –2.6 (metal-poor type-II supernovae, SNe II), [Fe/H] = –1.1 (SNe II + AGB stars), and [Fe/H] = –0.5 (SNe II + AGB + SNe Ia). Predictions at [Fe/H] = –0.5 for the halo and bulge components are also reported in the figure. The interstellar ¹²C/¹³C, ¹⁴N/¹⁵N, and ¹⁶O/¹⁸O ratios are difficult to measure in general, mainly because of their relatively high values that result in either high opacity for lines of the most abundant isotopologues or sensitivity problems for lines of the rarest isotopologues. To alleviate these problems, we normalized the ¹⁴N/¹⁵N and ¹⁶O/¹⁸O ratios by ¹²C/¹³C, considering the double-ratio obtained from, for example H¹³CN/HC¹⁵N or H¹³CO⁺/HC¹⁸O⁺ (see Muller et al. 2011). Hence, all the ratios for the $z = 0.89$ absorber in Fig. 2 are measured through optically thin lines and are therefore reliable.

All the ratios measured at $z = 0.89$ (SW), including ³⁵Cl/³⁷Cl, agree very well with the predictions by Kobayashi et al. (2011) for the solar neighbourhood at [Fe/H] = –2.6, except those of silicon and sulfur. This discrepancy should be viewed as an interesting constraint for chemical evolution models.

4. Summary and conclusions

The chloronium ion, H₂Cl⁺, was detected in the $z = 0.89$ absorber toward the lensed blazar PKS 1830–211. The H₂Cl⁺ relative abundance along the NE line of sight was found to be enhanced by a factor ~7 with respect to the SW line of sight. Since the NE line of sight is thought to be more diffuse, with a lower molecular gas fraction (H₂/H), this suggests that H₂Cl⁺ is a good tracer of the diffuse gas component. Toward the SW image, at a look-back time of more than half the present age of the Universe, we measured a ³⁵Cl/³⁷Cl isotopic ratio of 3.1^{+0.3}_{-0.2}, identical to its value in the solar system within the uncertainty, and within the range of values found in Galactic sources. Slightly deeper observations are expected to allow us to measure the ³⁵Cl/³⁷Cl ratio in the NE line of sight, that is, at a larger galactocentric radius in the

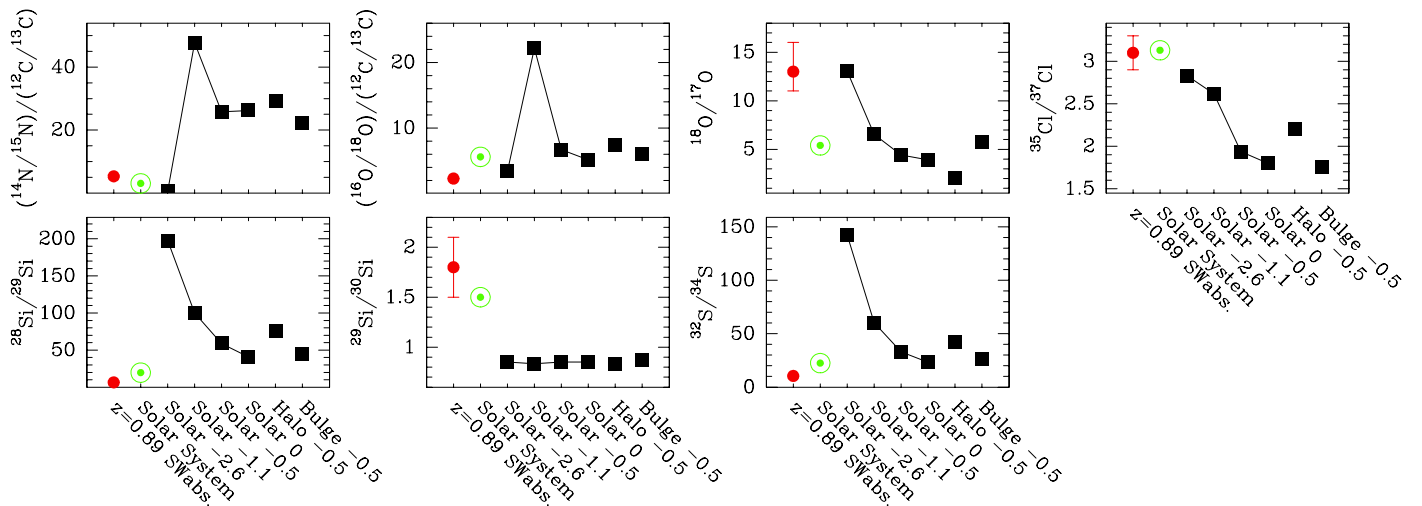


Fig. 2. Comparison of the isotopic ratios of C, N, O, S, Si, and Cl measured at $z = 0.89$ toward PKS 1830–211(SW) (Muller et al. 2006, 2011, 2013 and this work) and in the solar system (solar symbols in green, Lodders 2003), and predictions from evolution models from Kobayashi et al. (2011) (black squares) for the solar neighbourhood (solar, at $[\text{Fe}/\text{H}] = -2.6, -1.1,$ and -0.5), and halo and bulge at $[\text{Fe}/\text{H}] = -0.5$. The $^{14}\text{N}/^{15}\text{N}$ and $^{16}\text{O}/^{18}\text{O}$ ratios are normalized by the $^{12}\text{C}/^{13}\text{C}$ ratio, because of the difficulties of measuring all three separately in the $z = 0.89$ absorber toward PKS 1830–211.

absorber, which will provide an additional interesting constraint for chemical evolution models.

The detection of H_2Cl^+ toward PKS 1830–211 suggests that other chlorine-bearing species might be easily detectable (e.g., with ALMA), in particular hydrogen chloride, HCl. Future observations of other hydrides, such as CH^+ , OH^+ , H_2O^+ , HF, or ArH^+ , will provide more information on the conditions in this (so far unique) extragalactic molecular absorber.

Acknowledgements. This paper makes use of the following ALMA data: ADS/JAO.ALMA#2011.0.00405.S. ALMA is a partnership of ESO (representing its member states), NSF (USA) and NINS (Japan), together with NRC (Canada) and NSC and ASIAA (Taiwan), in cooperation with the Republic of Chile. The Joint ALMA Observatory is operated by ESO, AUI/NRAO and NAOJ. The financial support to Dinh-V-Trung from Vietnam's National Foundation for Science and Technology (NAFOSTED) under contract 103.08-2010.26 is gratefully acknowledged.

References

- Araki, M., Furuya, T., & Saito, S. 2001, *J. Mol. Spectr.*, 210, 132
 Blake, G. A., Keene, J., & Phillips, T. G. 1985, *ApJ*, 295, 501
 Cernicharo, J., & Guélin, M. 1987, *A&A*, 183, L10
 Cernicharo, J., Guélin, M., & Kahane, C. 2000, *A&AS*, 142, 181
 Cernicharo, J., Goicoechea, J. R., Daniel, F., et al. 2010, *A&A*, 518, L115
 De Luca, M., Gupta, H., Neufeld, D., et al. 2012, *ApJ*, 751, L37
 Flagey, N., Goldsmith, P. F., Lis, D. C., et al. 2013, *ApJ*, 762, 11

- Gerin, M., de Luca, M., Black, J., et al. 2010, *A&A*, 518, L110
 Gerin, M., de Luca, M., Lis, D. C., et al. 2013, *J. Phys. Chem. A*, 117, 10018
 Godard, B., Falgarone, E., Gerin, M., et al. 2012, *A&A*, 540, A87
 Goto, M., Usuda, T., Geballe, T. R., et al. 2013, *A&A*, 558, A5
 Kahane, C., Dufour, E., Busso, M., et al. 2000, *A&A*, 357, 669
 Kobayashi, C., Karakas, A. I., & Umeda, H. 2011, *MNRAS*, 414, 3231
 Koopmans, L. V. E., & de Bruyn, A. G. 2005, *MNRAS*, 360, L6
 Lellouch, E., Paubert, G., Moses, J. I., Schneider, N. M., & Strobel, D. F. 2003, *Nature*, 421, 45
 Lodders, K. 2003, *ApJ*, 591, 1220
 Lis, D. C., Pearson, J. C., & Neufeld, D. A. 2010, *A&A*, 521, L9
 Martí-Vidal, I., Vlemmings, W., Muller, S., & Casey, S. 2014, *A&A*, 563, A136
 Monje, R. R., Lis, D. C., Roueff, E., et al. 2013, *ApJ*, 767, 81
 Moullet, A., Gurwell, M. A., Lellouch, E., & Moreno, R. 2010, *Icarus*, 208, 353
 Moullet, A., Lellouch, E., Moreno, R., et al. 2013, *ApJ*, 776, 32
 Muller, S., & Guélin, M. 2008, *A&A*, 491, 739
 Muller, S., Guélin, M., Dumke, M., et al. 2006, *A&A*, 458, 417
 Muller, S., Beelen, A., Guélin, M., et al. 2011, *A&A*, 535, A103
 Muller, S., Beelen, A., Black, J. H., et al. 2013, *A&A*, 551, A109
 Muller, S., Combes, F., Guélin, M., et al. 2014, *A&A*, 566, A112 (Paper I)
 Müller, H. S. P. 2008, *The Cologne Database for Spectroscopy*, unpublished result (<http://www.astro.uni-koeln.de/cdms>)
 Neufeld, D. A., & Wolfire, M. G. 2009, *ApJ*, 706, 1594
 Neufeld, D. A., Roueff, E., Snell, R. L., et al. 2012, *ApJ*, 748, 37
 Peng, R., Yoshida, H., Chamberlin, R. A., et al. 2010, *ApJ*, 723, 218
 Qin, S.-L., Schilke, P., Comito, C., et al. 2010, 521, L14
 Salez, M., Frerking, M. A., & Langer, W. D. 1996, *ApJ*, 467, 708
 Schilke, P., Neufeld, D. A., Müller, H. S. P., et al. 2014, *A&A*, 566, A29
 Thielemann, F. K., & Arnett, W. D. 1985, *ApJ*, 295, 604